

THE EFFECT OF STRUCTURAL DISCONTINUITY ON ANTISYMMETRIC RESPONSE OF A CONTAINER SHIP

S.E. Hirdaris^a, S. H. Miao^b and P. Temarel^b

^a Strategic Research Group, Lloyd's Register, UK

^b Ship Science, School of Engineering Sciences, University of Southampton, UK

ABSTRACT

Recent trends in capacity, hence size, growth in container ships have increased the importance of torsion, particularly how it is influenced by the large deck openings and structural discontinuities present in such ships. This paper investigates the consequences of these effects on the 'dry' antisymmetric modal characteristics and consequent wave-induced loads. A beam model with more accurate representation of warping and structural discontinuities is applied to a box beam to assess these influences and compare predictions of natural frequencies and mode shapes with previous calculations and finite element (FE) predictions. The analysis is subsequently applied to a feeder containership travelling in regular oblique waves and resultant loads are compared with predictions obtained from previous two (2D) - and three-dimensional (3D) hydroelasticity analyses.

KEYWORDS

Antisymmetric; beam; containership; hydroelasticity; large opening; structural discontinuity

1. INTRODUCTION

The wave-induced structural response of ships with large openings, such as containerships, especially for torsion, is of importance to the designer, particularly due to recent trends for larger ships. There are a number of issues to consider: (i) the flexural direct stress, due to bending, is augmented with sectorial direct stress induced by constrained cross-sectional warping; (ii) when using 2D hydroelasticity, the structural discontinuity at the transitions between open and closed parts of the ship results in changes to its antisymmetric (coupled horizontal bending and torsion) dynamic characteristics, such as natural frequencies and principal modes, by comparison to 2D analyses which do not take into account structural discontinuities¹. Past investigations on a bulk carrier and a containership, comparing 2D and 3D predictions using hydroelasticity analysis, showed differences for the torsional moment obtained using beam and 3D FE structural idealisations²⁻⁴. On the other hand such differences were not observed in similar comparisons carried out for a mine hunter, a ship without any significant deck openings or structural discontinuities⁵.

The Timoshenko beam theory used previously for coupled horizontal bending and torsion^{6,7} is modified by treating the warping as an independent variable as well as accounting for the abrupt changes in cross-sectional properties occurring at the transition areas between open and closed

parts of the ship¹. The finite difference method is used to obtain natural frequencies and principal modes of the 'dry' hull. The methodology developed is validated for a simple box beam with one deck opening by comparing current predictions with 3D FE results and previous predictions^{1,6}. Subsequently the method is applied to a 750 TEU feeder container ship. The influence of accounting for structural discontinuities of ships with large deck openings is assessed by comparing current predictions for dry hull dynamic characteristics and regular wave-induced loads with previous 2D predictions, not including this influence, and 3D results⁴. A by-product of this paper relates to finite element modelling of the ship's structure, and generating FE models suitable to simulate the global dynamic behaviour of ships.

2. THEORETICAL BACKGROUND

Bishop et al⁷ developed a beam theory to include the coupling of horizontal bending and torsion of beam-like structures. There are three independent variables in their theory, namely horizontal displacement (of shear centre^{6,7}) v , angle of twist ϕ and rotation θ about the vertical axis of the cross-section. Furthermore in their theory warping of the cross-section is proportional to the first derivative of the twist angle, namely $\chi = \phi'$. That is to say the longitudinal displacement induced by torsion at a point of the cross-section is $u = -w\phi'$, where w is the so called sectorial coordinate. In the theoretical model by Pedersen¹, which is adopted in this paper, warping is treated as an independent variable; hence the longitudinal displacement induced by torsion is $u = -w\chi$.

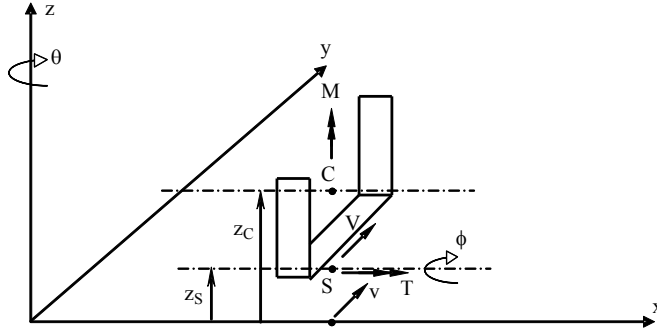


Figure 1: Global coordinate system used in the current analysis

The equations of motion used in this paper are based on the coordinate system shown in Fig. 1. The equations of motion for the (coupled) horizontal displacement and rotation about vertical axis are similar to those by Bishop and Price, namely

$$V'(x,t) = \mu(x)[\ddot{v}(x,t) - z_C(x)\ddot{\phi}(x,t)], \quad (1)$$

$$I_z(x)\ddot{\phi}(x,t) = M'(x,t) + V(x,t), \quad (2)$$

where v denotes the horizontal displacement at the base line, μ is mass per unit length, I_z rotatory inertia, V horizontal shear force, M horizontal bending moment and z_C is shown in Fig.1. An overdot denotes derivative with respect to time and a prime with respect to distance x along the structure. The relationships between horizontal displacement and shear strain, and for the horizontal bending moment and shear force, when using Timoshenko beam theory are as follows:

$$v'(x,t) = \theta(x,t) + \gamma(x,t) + [z_S(x)\phi(x,t)]', \quad (3)$$

$$M(x,t) = EI(x)\theta'(x,t), \quad (4)$$

$$V(x,t) = kAG(x)\{v'(x,t) - \theta(x,t) - [z_S(x)\phi(x,t)]'\} + GI_{ph}(x)[\phi'(x,t) - \chi(x,t)], \quad (5)$$

where γ denotes the shear strain, E Young's modulus, $I=I_{yy}$ second moment of area, G shear modulus, kA effective shear area, I_{ph} shear area moment and z_S is shown in Fig.1. The last term in Eq.(3) and the last two terms in Eq.(5) are not included in the theoretical model used by Bishop et al¹. The equation of motion for the (coupled) angle of twist is

$$T'(x,t) = [I_C(x) + \mu(x)\bar{z}(x)z_C(x)]\ddot{\phi}(x,t) - \mu(x)\bar{z}(x)\ddot{v}(x,t), \quad (6)$$

where T denotes the twisting moment, I_C the moment of inertia per unit length, about the longitudinal axis, and $\bar{z}(x)=z_C(x)-z_S(x)$. This equation is similar to that used by Bishop and Price, accounting for the different coordinate system. As a result of the use of warping χ as an independent variable, the twisting moment can be written as

$$\begin{aligned} T(x,t) &= C(x)\phi'(x,t) + G[I_{hh}(x) - J(x)][\phi'(x,t) - \chi(x,t)] + G I_{ph}(x) \gamma(x,t) \\ &= C(x)\phi'(x,t) - [C_w(x)\chi'(x,t)] \end{aligned} \quad (7)$$

where $C=GJ$, with J denoting the torsional constant, $C_w=EI_{ww}$, with I_{ww} denoting the sectorial moment of inertia (or warping constant) and I_{hh} the warping rotational moment of inertia. The second line in Eq.(7) is the same as in the previous theoretical model, provided $\chi=\phi'$ is assumed^{6,7}. Finally the bimoment can be expressed as

$$B(x,t) = -C_w(x)\chi'(x,t). \quad (8)$$

A finite difference method is adopted in order to obtain natural frequencies and modal characteristics for a beam with both ends free. This follows the same procedure adopted before, satisfying the boundary conditions for zero horizontal bending moment, horizontal shear force and torsional moment at both ends^{6,7}. One final boundary condition relates to warping, namely

$$C_w(x)\chi'(x) + K(x)\chi(x) = 0 \quad (9)$$

at both ends of the beam, namely $x=0$ and $x=L$. In Eq.(9) K denotes a warping stiffness constant, constant, whose value is difficult to establish; hence, $K=0$ is used in this paper. The previous method uses a more simplified boundary condition in place of Eq.(9), namely ($\phi''=0$) at $x=0$ and L .

In order to successfully deal with structural discontinuities, and their effects on natural frequencies and mode shapes, Pedersen also introduced bending and warping compatibility factors at the points along the beam where abrupt changes in cross-sectional properties occur. The warping compatibility factor S_1 is given as

$$S_1 = \sqrt{\left[I_{ww}^- - \frac{(I_{yw}^-)^2}{I_{yy}} \right] \left[I_{ww}^+ - \frac{(I_{yw}^+)^2}{I_{yy}} \right]^{-1}} \quad (10)$$

and the bending compatibility factor S_2 is given by

$$S_2 = \left(I_{yw}^- - S_1 I_{yw}^+ \right) (I_{yy})^{-1}. \quad (11)$$

In these equations I_{yw} denotes the bending-warping coupling moment of inertia, and the + and - signs denote the cross-section properties at either side of the discontinuity. It should be noted that although horizontal bending moment and shear force are not directly affected by the discontinuity, the twisting moment and bimoment are different either side of the discontinuity, the former depending on the position of the shear centre S and the horizontal shear force, the latter depending on the compatibility factors and the horizontal bending moment.

3. VALIDATION OF MATHEMATICAL MODEL

The box beam used by Pedersen was adopted for validation of the mathematical model of the previous section. This beam, shown in Fig. 2(a), is 2.4m long (L), 0.4m wide and 0.2m high, with a rectangular hollowed out shape resulting in wall thickness of 0.3mm made of steel. The top (or deck) plating is taken off for the middle 1.2m of the beam, providing a good example of structural discontinuity. It should also be noted that the ends of the beam are also hollow. The sectional structural properties are summarised in Table 1, both for the open and closed sections.

TABLE 1
SUMMARY OF THE MAIN PROPERTIES OF THE BOX BEAM

	Closed	Open		Closed	Open
μ (tonnes/m)	0.02826	0.01884	J (m^4)	6.4E-05	0.72E-08
I (m^4)	7.787E-05	6.400E-05	I_w (m^6)	5.33E-08	28.0E-8
kA (m^2)	0.0024	0.0012	I_{hh} (m^4)	7.2E-05	5.5E-05
I_C (tonnes m^2/m)	8.227E-04	5.809E-04	I_{ph} (m^3)	0.0	9.0E-05
z_C, z_S (m)	0.1, 0.1	0.05, -0.075	I_{yw} (m^5)*	-5.3E-07	0.0

* integration carried out over the common area at the discontinuity.

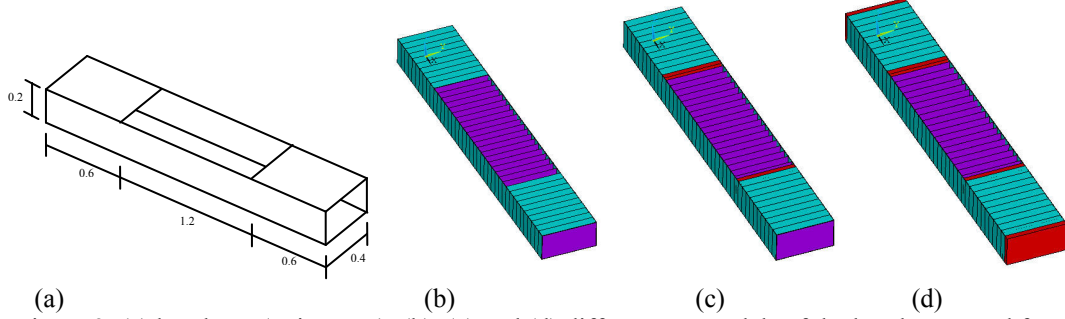


Figure 2: (a) box beam(unit metre); (b), (c) and (d) different FE models of the box beam used for validation

Variations on the mathematical model described in the previous section were carried out, in order to fine-tune the influence of certain parameters. The following models were used:

- Model A corresponds to the original method^{6,7}, with differences in Eqs.(3), (5), (7), (8) and (9) indicated in section 2; naturally this model does not account for structural discontinuities, except through the structural properties;
- Model B adopts the equations in section 2; however, the influence of the shear strain is omitted when evaluating the horizontal displacement and twist from Eqs.(3) and (7), respectively;
- Model C adopts the equations in section 2; in addition the shear strain γ and the rate of twist angle ϕ' are reevaluated at the structural discontinuity due to changes in the torsional moment.
- Model C1 adopts the same equations as model C, but without reevaluating γ and ϕ' at the structural discontinuity.

The first 3 natural frequencies for this box beam are shown in Table 2. Modes $r=0, 1$ and 2 correspond to the rigid body modes of sway, yaw and roll, respectively. PTD denotes the predictions by Pedersen¹. Case (D) denotes using the compatibility factors given by Eqs.(10) and (11), thus allowing for the effects of structural discontinuity. In this case, using the properties of closed and open cross-sections, $S_1=1/3$, $S_2=-1/120$ from the closed to the open cross section, and $S_1=3$, $S_2=1/40$ from open to closed cross-section. Case (WD) in Table 2 denotes the case where the influence of structural discontinuities was neglected, implying $S_1=1$, $S_2=0$ from closed to open cross section, and $S_1=1$, $S_2=0$ vice versa. 20 and 80 sections along the box beam were used. The relevant number of sections is indicated in Table 2. The dominant distortion in each mode is indicated, T for torsion and HB for horizontal bending together with the number of nodes.

TABLE 2
NATURAL FREQUENCIES OF THE BOX BEAM (RAD/S)

Modal index r	PTD (D)	model A (80)	model B (D; 80)	model C (D; 80)	model C1 (D; 80)	model B (D; 20)	model C (D; 20)	model C1 (D; 20)
3(1T)	862	763	884	860	857	892	876	865
4(2HB)	2359	2482	2335	2293	2296	2352	2317	2323
5(2T)	3845	3754	3784	3567	3552	3851	3651	3598

Modal index r	PTD (WD)	model C1 (WD; 20)	FE 1	FE 2	FE 3	FE 4	FE 5
3(1T)	500	608	677	770	824	892	896
4(2HB)	2058	2183	1963	2241	2357	2367	2368
5(2T)	3348	3317	3117	3403	3635	3809	3856

As can be seen from Table 2 model A predicts lower natural frequencies by comparison with Pedersen's¹ results, except for the horizontal bending dominant mode. Model B, with 80 sections and for case (D), provides good overall predictions with a small overestimate for mode $r=3$; however, when 20 sections are used the predicted natural frequencies increase (by less than 10% for the first two modes), but still there is good agreement with Pedersen's predictions. Models C and C1, with 80 sections and for case (D), provide good predictions for mode $r=3$, but smaller natural frequencies for modes $r=4$ and 5 , about 3% and 8% smaller than Pedersen's predictions. Decreasing the number of sections used results in increasing these predictions. Predicted natural frequencies when the effects of structural discontinuities are neglected, i.e. case (WD), are also shown in Table 2. All predictions are lower than all the other models, especially for the torsion dominant modes $r=3$ and 5 , including model A. This tends to show that simply treating the warping function as an independent variable is not sufficient at all, and the effects of structural discontinuities need to be included.

Previous applications of 3D hydroelasticity used shell finite elements²⁻⁵. It is, therefore, important to compare current predictions, with those from a suitable FE model. The basis FE model comprises 40 sections along the beam, each 0.06m long. This is shown in Fig.2(b) and, as can be seen, also contains 41 fictitious bulkheads of thickness t_{fb} . Shell 63 elements are used, allowing for membrane effects only. A total 181 (140 for the structure and 41 for the fictitious bulkheads) elements are used. The fictitious bulkheads are used in order to eliminate mode shapes which involve the distortion of the cross-section, which is not admissible within a beam theory. Three sets of results are shown in Table 2 with FE1, FE2 and FE3 corresponding to $t_{fb}=0.1, 0.5$ and 3 mm, respectively. As expected, the natural frequencies predicted by these 3 FE models increase with increasing t_{fb} . This observation is consistent with Vlasov's thin-walled beam theory⁸. However, even when using fictitious bulkheads as thick as the box beams walls (i.e. 3mm) results in natural frequencies that are, in general, smaller than any of the beam models accounting for the effects of structural discontinuities. It should be emphasized that the aim of these comparisons is to constrain the 3D FE model to behave as much as possible like a beam, in order to assess the influence of the discontinuities, as well as that of warping. A slightly different approach was

formulated with the aim of keeping the fictitious bulkhead thickness at acceptably low levels. Accordingly model FE4 has $t_{fb}=0.1\text{mm}$, as per model FE1, for all fictitious bulkheads except those at the edge of the open top (or deck). These are set at 65mm, together with allowing for bending as well as membrane effects (see Fig.2(c)). As can be seen from Table 2, the predictions from model FE4 are very close to beam theory predictions for modes $r=4$ and 5, but overestimate a little for mode $r=3$, the first distortion torsion dominant mode. Finally model FE5 is as per FE4, with the addition of two 65mm thick fictitious bulkheads at the ends of the box beam, as can be seen in Fig.2(d). The natural frequencies predicted by FE5 are higher than FE4, especially for the torsion dominant mode $r=5$. It can thus be seen that the thickness of the fictitious bulkheads in way of discontinuities is very influential in the 3D FE models predicting natural frequencies for the torsion dominant modes close to those obtained from suitable beam models.

The modal horizontal displacement (at the shear centre), twist angle and warping function, all normalised for 1m horizontal displacement at stern, are shown in Fig.3 for the torsion and horizontal bending dominant modes, $r=3$ and 4, respectively. Results from the finite element model FE 5 are also shown.

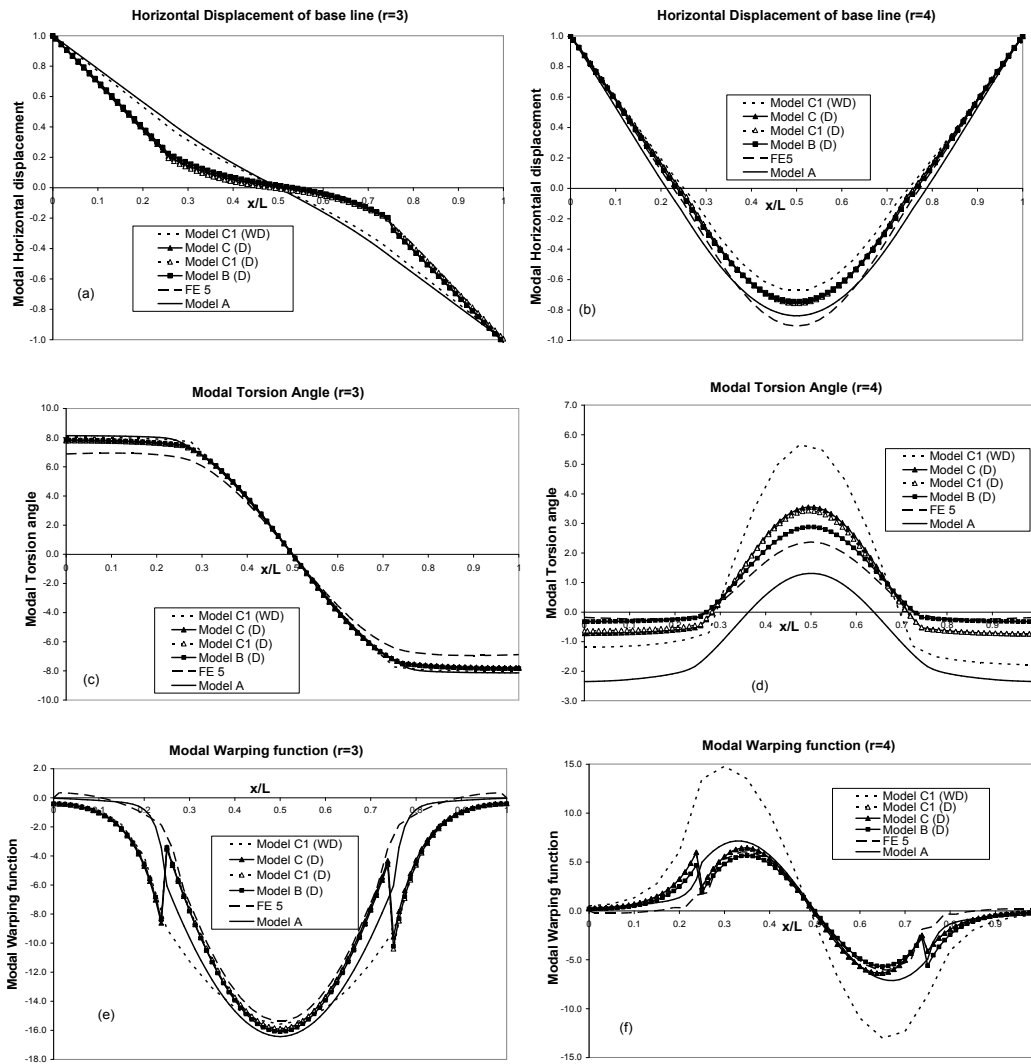


Figure 3: Modal properties for the box beam; (a, b) horizontal displacement (m); (c, d) twist (rad); (e, f) warping (rad/m); modes $r=3$ (a, c, e) and 4 (b, d, f)

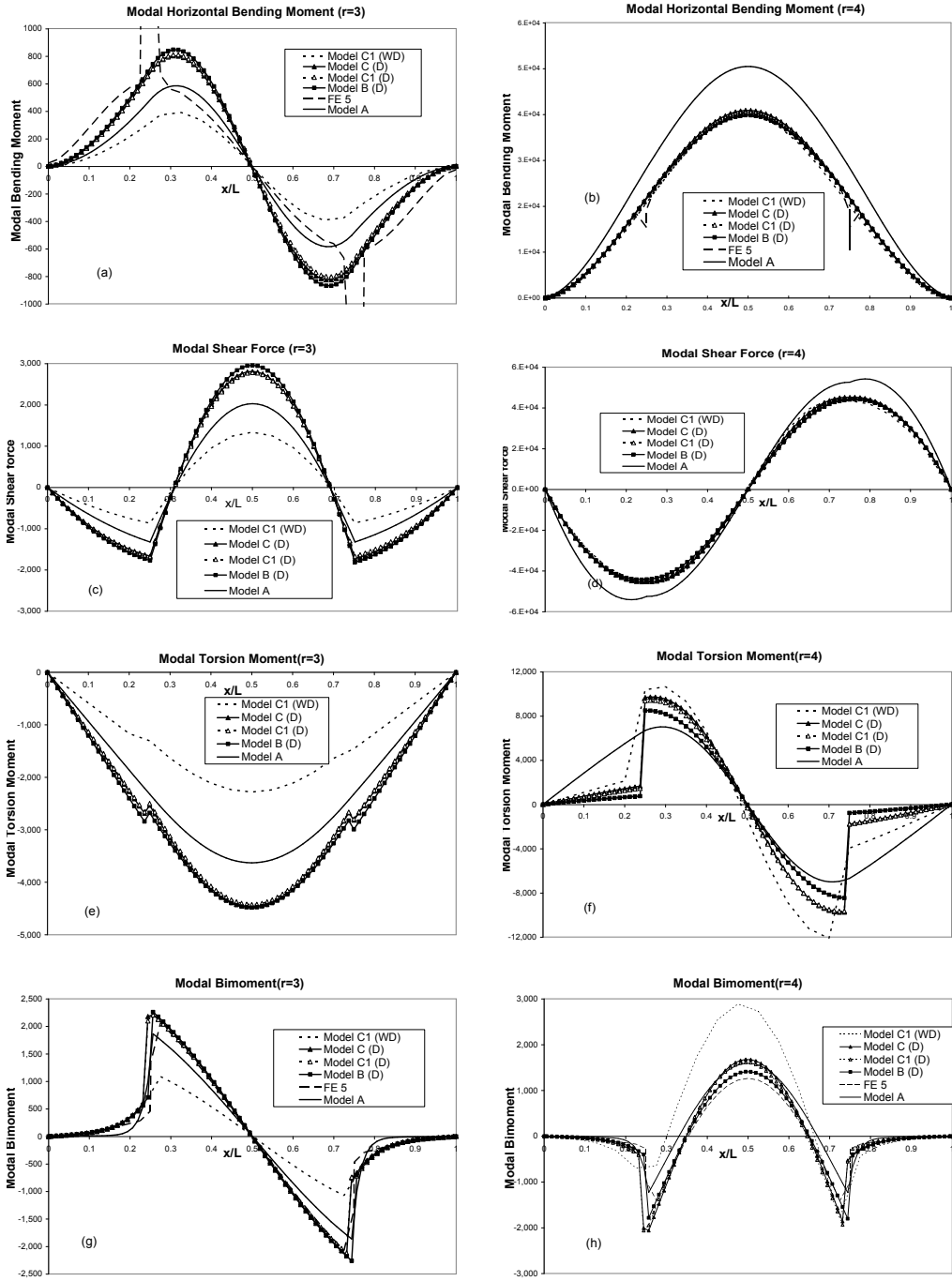


Figure 4: Modal internal actions for box beam; (a, b) HBM (kNm); (c, d); HSF (kN); (e, f) TM (kNm); (g, h) bimoment (kNm^2); modes $r=3$ (a, c, e, g) and 4 (b, d, f, h)

All models for case (D), including FE 5, result in very close modal horizontal displacement variations along the box beam for mode $r=3$. The influence of the structural discontinuity can be seen by a small kink in the mode shapes at $x/L=0.25$ and 0.75 . Model A and model C1, for case (WD), are different not reflecting the influence of structural discontinuities. All models show similar twist variation along the box beam for mode $r=3$, which is relatively smooth. FE 5 is

slightly smaller than the rest. Interestingly the only kinks in the twist variation along the beam are noted for model C1, case (WD). Similarly for the modal warping function for $r=3$ models B, C and C1, for case (D), are close to each other and reflect the structural discontinuity rather sharply. When these effects are excluded the warping function varies rather smoothly along the beam, i.e. model A and C1, case (WD). It is interesting to note that the predictions evaluated from the FE model, based on the relationship between sectorial direct stress and the bimoment, also show smooth variation. Larger differences between the various models are observed for the horizontal bending dominant mode $r=4$, especially for case (WD). This is more apparent in the modal twist and warping function. Nevertheless the modal characteristics predicted by models B, C, C1 and FE 5 are reasonably close to each other for mode $r=4$. Interestingly model A results in comparable variations for v_4 and χ_4 , but not ϕ_4 .

Modal internal actions, namely horizontal bending moment (HBM), horizontal shear force (HSF), torsional moment (TM) and bimoment (BM), for modes $r=3$ and 4 are shown in Fig.4. As can be seen models B, C and C1, for case (D), produce similar variations along the box beam and reflect the presence of the structural discontinuities for TM and BM. The predicted modal internal actions by models B, C and C1, case (D), are very close for $r=3$, but show small differences for $r=4$. When this influence is ignored, i.e. model C1 case (WD), differences are observed for all internal actions for the twisting dominant mode $r=3$, but there is good agreement for the bending dominant mode $r=4$. It is interesting to note, however, that model A provides predictions that are in between cases (D) and (WD) for $r=3$ and comparative, but larger, predictions to case (D) for HBM and HSF and smaller predictions for TM, for $r=4$, without reflecting the influence of structural discontinuities for the latter. Predictions for BM are also included for model FE 5, using the sectorial direct stress, showing good agreement with models B, C and C1 for case (D). There is also good agreement for the HBM values evaluated from the direct stress distribution of the FE model for both $r=3$ and 4; however, as can be seen from Figs.4(a,b), the FE based prediction using FE 5, with rather thick fictitious bulkheads at the location of the discontinuity, result in large kinks for the modal HBM for the twisting dominant mode $r=3$ and even the horizontal bending dominant mode $r=4$. FE predictions are not included for HSF and TM as the shear stress distributions are not accurate enough for this relatively crude model. It should also be noted that model A provides good estimates for the bimoment, using $B = -EI_w\phi''$, for either $r=3$ or 4.

Figs.3 and 4 show some interesting aspects regarding the influence of structural discontinuities and the influence of the compatibility factors, given by Eqs.(10, 11). These are excluded for model C1 (WD) and naturally model A. One can see their effects clearly in the warping function of Fig.4 (e,f); however, they only appear to influence the horizontal displacement of the twisting dominant mode ($r=3$) and the twist of the horizontal bending dominant mode ($r=4$). A pattern may also be discerned for the internal actions, namely all of them are affected in the torsion dominant mode ($r=3$), but not particularly affected in the horizontal bending dominant mode ($r=4$), with the exception of model A in the latter case. It is, therefore, difficult to draw any hard and fast conclusions even for the simple case of a box beam.

4. APPLICATION TO A FEEDER CONTAINERSHIP

As an application the aforementioned mathematical models are applied to the feeder (750 TEU) containership, shown in Fig.5(a), previously investigated by Basaran et al⁴. Its principal dimensions are: length $L_{pp}=L=124.9\text{m}$, beam $B=20.8\text{m}$, depth $D=10.4\text{m}$. The condition investigated here corresponds to what is referred to as Model 1 by Basaran et al⁴, with $\Delta=19623$ tonnes and draught $T=9\text{m}$. The variation of the sectorial moment of inertia (or warping constant) I_{ww} and torsional constant J are shown in Figs.5(b, c), indicating that the structural data account for the discontinuities in the deck plating. Please note that there are two sets of data for I_{ww} and J , denoted by A and B; the former (A) considers the structure between the main holds whilst the latter (B) treats the entire hold area as a continuous open deck.

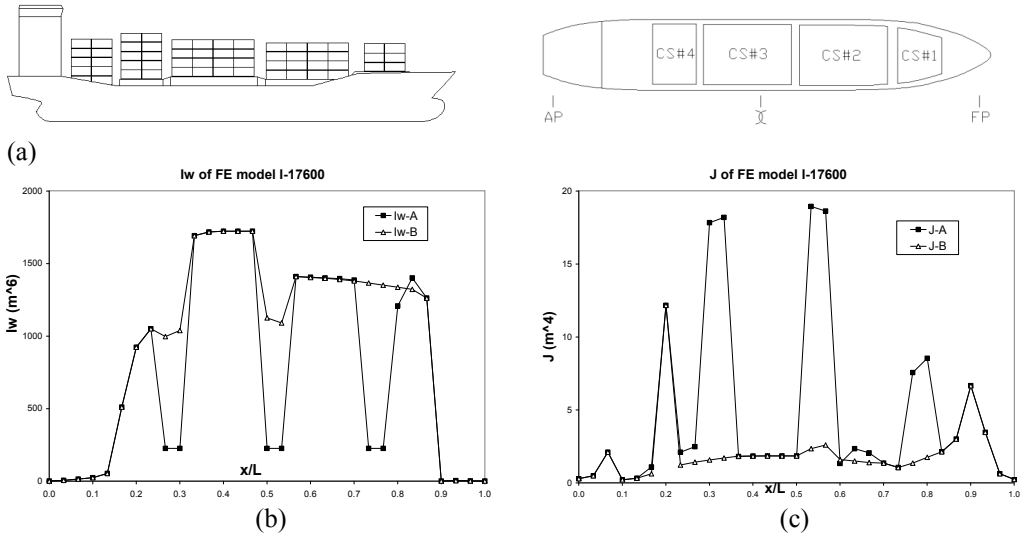


Figure 5: (a) General arrangement, (b) warping and (c) torsional constants of the containership

TABLE 3
DRY HULL NATURAL FREQUENCIES OF THE FEEDER CONTAINERSHIP (RAD/S)

Modal index r	model A	model B (D)	model C (D)	model C1 (D)	model C1 (EI _w -B) (D)	model C1 (WD)	3D FE ⁴
3 (1T)	6.51	7.45	5.80	5.77	6.25	5.56	7.82
4 (2T)	10.77	10.45	9.22	9.01	10.00	9.09	11.88
5 (3T)	17.27	15.86	13.52	13.25	14.99	13.99	20.53
6 (2HB)	19.46	22.79	18.65	18.79	19.86	18.94	26.01
7 (4T)	26.92	28.48	26.20	25.75	26.60	22.90	29.94

The structure was idealised using 30 sections along the containership. The same mathematical/numerical model definitions, given in section 3, are used. For models B, C and C1 the compatibility factors S_1 and S_2 were evaluated at the discontinuities, identified based on the variation of the position of the shear centre. The dry hull natural frequencies are shown in Table 3. All of models A, B, C and C1 use the I_{ww} -A and J-A set of properties, shown in Fig. 5. There is an additional set of dry hull natural frequencies for model C1, denoted by (EI_w-B), using the I_{ww} -B and J-A set of properties, shown in Fig.5. Results obtained by Basaran et al⁴ using a 3D FE idealisation, comprising 6966 shell63 finite elements, are also included in Table 3. This is a relatively detailed FE model; hence, the use of fictitious bulkheads is limited to the common frames in the region of the intermediate decks between the double skins. The FE model also includes the structure in way of the hatch coamings, as well as deck cargo using lump mass elements. The dominant mode is indicated in brackets, including the number of nodes. Natural frequencies predicted by models C and C1 are lower than those of model A. This is in line with what has been observed in the box beam (see Table 2), except for the first torsion dominant mode. Furthermore natural frequencies obtained from model B, are higher than those for models C and C1, similar to the trends observed in the box beam albeit showing larger differences. Model B appears to provide the closest set of natural frequencies to the results of the FE model. It should be noted, however, that the FE models experiences some regional distortions from around 20 rad/s, most probably due to the use of lump mass elements. Use of model C1 (EI_w-B) results in higher natural frequencies, broadly comparable to those predicted by model B. The choice of apparently inconsistent properties, namely EI_w-B and J-A, deserves an explanation. If we were to use the set EI_w-B and J-B, that would have resulted in the ship being too flexible from a twisting point of view and a much lower dry hull natural frequency for the first, twisting-dominant, mode. The

natural frequencies obtained for the C1 (EI_w-B) case indicate that the structure between the holds is very important from a torsion point of view when using a beam idealisation. Ignoring the effects of structural discontinuities, i.e. case (WD) for model C1, results in smaller natural frequencies, as can be seen from Table 2. Model A provides a set of natural frequencies sufficiently close to the FE predictions.

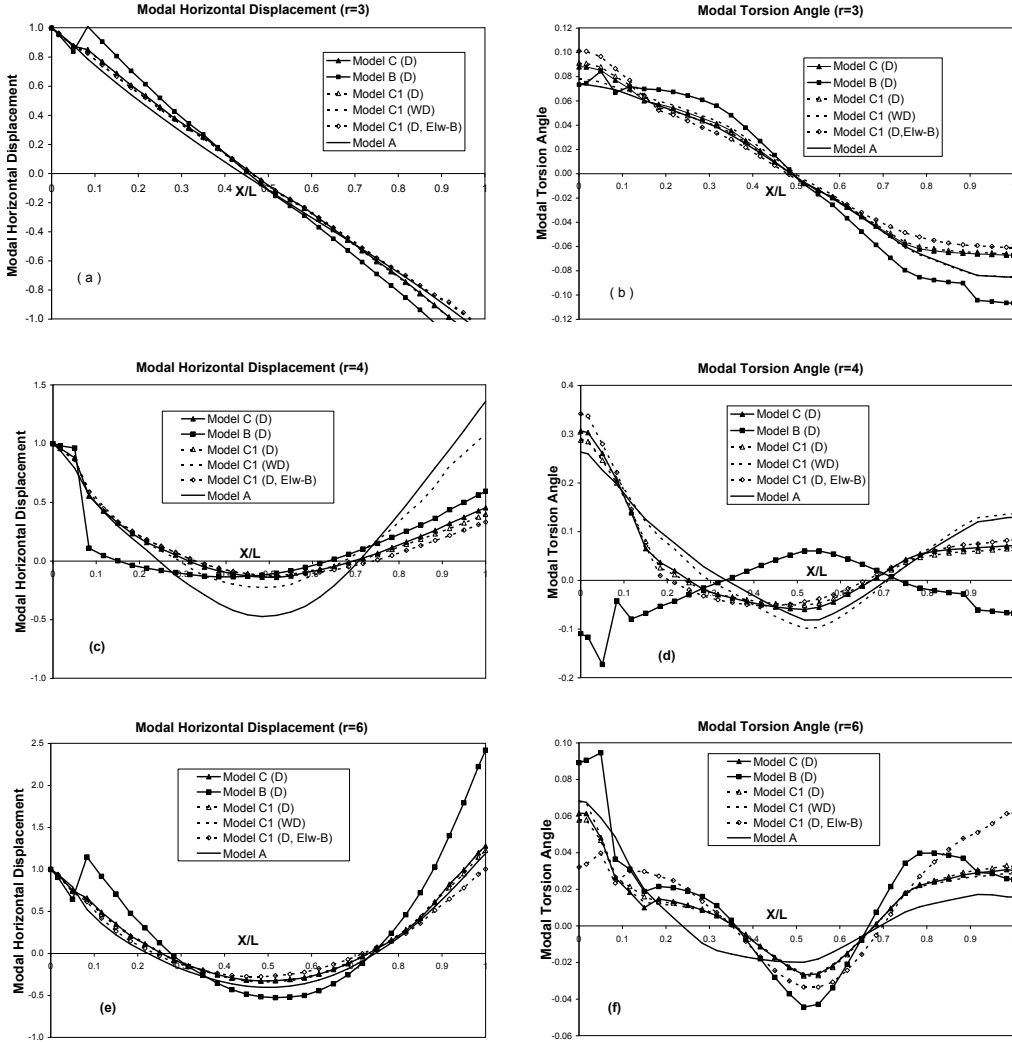


Figure 6: Modal horizontal displacement(m) and twist (rad) for the feeder container ship (a, b) $r=3$; (c, d) $r=4$; (e, f) $r=6$.

The modal horizontal displacement at the shear centre and twist for modes, $r=3$, 4 and 6, are shown in Fig.6. There is good correlation, in general, between all models used for $r=3$. The influence of ignoring the effect of structural discontinuities, i.e. models A and C1 (WD), can be discerned for $r=4$ in Figs.6(c,d). The correlation is good enough even when the modal complexity increases as in the case for $r=6$, the horizontal bending dominant mode. There is concern with reference to the predicted mode shapes for $r=4$ when using model B, e.g. see Fig.6(d).

The dynamic behaviour of the feeder containership was examined when travelling at 8.23 m/s in regular waves of 1m amplitude, encountered at 135° heading. The equations of motion, evaluation of principal coordinates and the prediction of bending moments, shear forces etc using

modal summation is very well known^{6,7}; hence not repeated here. The variation of HBM, HSF, TM and BM along the ship predicted by models A, B, C and C1 are shown in Fig.7, for a regular wave of frequency 0.72 rad/s, $L/\lambda=1.04$, λ being the wave length. As can be seen the use of mathematical models with small differences between them does not appear to affect the horizontal bending moment and, by and large, the horizontal shear force. The same observation is also valid for TM, with model A providing the lowest predictions. On the other hand there is more difference between the bimoment distributions predicted by the various models. Furthermore the bimoment has a rather jagged variation, reflecting the discontinuities along the containership (see Fig.5). Variations of wave-induced loads along the ship were not calculated using the 3D FE model. Previous comparisons between model A and the 3D FE model indicated that the former underestimated, by and large, compared to the latter⁴. It can, thus, be remarked that models B, C and C1 predict values which are likely to be closer to the 3D FE predictions. Nevertheless, the variations need to be compared with those of the FE model to justify this remark. An interesting aspect of the wave-induced loads shown in Fig.7, is the relative narrow range where the predictions from various models, with different sets of natural frequencies, fit in. This is an observation that needs to be confirmed by applications to other models of the same ship⁴ and other ships.

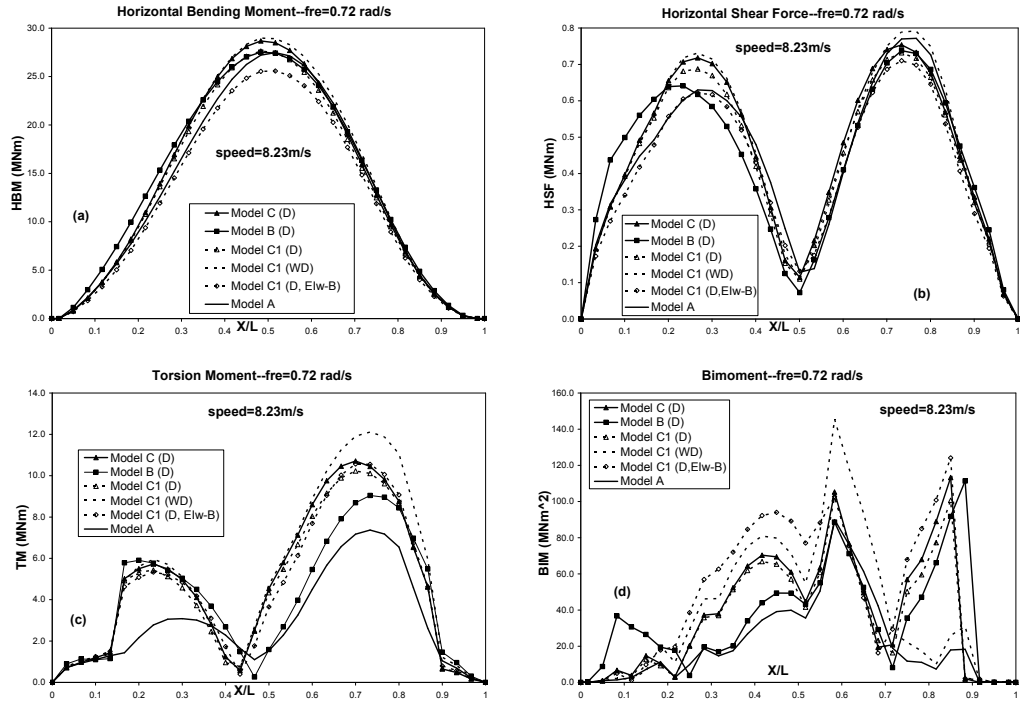


Figure 7: (a) Horizontal bending moment, (b) horizontal shear force, (c) torsional moment and (d) bimoment variation along the containership travelling at 8.23m/s in oblique (135° heading) regular waves of $L/\lambda=1.04$

5. CONCLUSIONS

A method for the dynamic analysis of beam-like ships with large deck openings and associated structural discontinuities has been illustrated using a box beam and a feeder containership, including wave-induced loads in oblique regular waves for the latter. Different numerical models were examined in order to assess the influence of the discontinuities and the effect of other

structural parameters. The following conclusions can be drawn from the investigations so far:

- Inclusion of structural discontinuities has an important influence on natural frequencies. This is also, in general, the case for corresponding mode shapes and modal internal actions; however, the effects vary and it is difficult to establish a pattern of influence in terms of torsion or bending dominant mode shapes or a particular modal characteristic.
- This is particularly evident in the case of the feeder containership, where any differences in the modal characteristics appear not to have small influence in the predicted antisymmetric wave-induced loads in waves of the same length as the ship. The torsional moment and bimoment appear to be the exceptions, which is to be expected.
- Making comparisons with predictions from 3D FE structural models is not particularly easy due to the fundamental differences in their structural behaviour, by comparison to beams. Nevertheless, it is believed that the applications in this paper provide useful guidance for verifying predictions for beam-like structures using 3D FE models.

Further work is required for confirming the observations made in this paper through applications to other types of ship with large deck openings, as well as comparisons with 3D FE structural models.

ACKNOWLEDGEMENTS

The authors acknowledge the support of the University of Southampton Lloyd's Register Educational Trust University Technology Centre. Dr. Hirdaris acknowledges the support of Lloyd's Register Marine Business.

"Lloyd's Register, its affiliates and subsidiaries and their respective officers, employees or agents are, individually and collectively, referred to in this clause as the 'Lloyd's Register Group'. The Lloyd's Register Group assumes no responsibility and shall not be liable to any person for any loss, damage or expense caused by reliance on the information or advice in this document or howsoever provided, unless that person has signed a contract with the relevant Lloyd's Register Group entity for the provision of this information or advice and that in this case any responsibility or liability is exclusively on the terms and conditions set out in that contract."

REFERENCES

1. Pedersen, P.T., A beam model for the torsional-bending response of ship hulls. *Trans. Royal Institution of Naval Architects*, 1983, 125, 171-182.
2. Hirdaris, S.E., Price, W.G. and Temarel, P., Two- and three-dimensional hydroelastic analysis of a bulker in waves. *Marine Structures*, 2002, 16, 627-658.
3. Hirdaris, S.E., Miao, S.H., Price, W.G and Temarel, P., The influence of structural modelling on the dynamic behaviour of a bulker in waves. *Proc. 4th Int. Conf. Hydroelasticity in Marine Technology*, 2006, 25-33, China.
4. Basaran, I., Belik, O. and Temarel, P., Dynamic behaviour of a containership using two- and three-dimensional hydroelasticity analyses. *Proc. 27th Int. Conf. on Offshore Mechanics and Arctic Engineering OMAE*, 2008, paper 57401, Portugal.
5. Price, W.G., Salas Inzunza, M. and Temarel, P., The dynamic behaviour of a mono-hull in oblique waves using two- and three-dimensional fluid structure interaction models. *Trans. Royal Institution of Naval Architects*, 2002, 144, 1-26.
6. Bishop, R.E.D. and Price, W.G., *Hydroelasticity of Ships*, Cambridge University Press, 1979.
7. Bishop, R.E.D., Price, W.G. and Temarel, P., A unified dynamic analysis of antisymmetric ship responses to waves. *Trans. Royal Institution of Naval Architects*, 1980, 122, 349-365.
8. Vlasov, V.Z., *Thin-Walled Elastic Beams*, Jerusalem, Israel Program for Scientific Translations Ltd, 1961.